Hindawi
Advances in Civil Engineering
Volume 2018, Article ID 3780482, 20 pages
https://doi.org/10.1155/2018/3780482

Review Article

An Overview of Methods for Blast Load Testing and Devices for Pressure Measurement

H. Draganić, D. Varevac, and S. Lukić

Faculty of Civil Engineering and Architecture Osijek, Josip Juraj Strossmayer University of Osijek, Vladimira Preloga 3, 31000 Osijek, Croatia

Correspondence should be addressed to H. Draganić; draganic@gfos.hr

Received 13 June 2018; Revised 18 September 2018; Accepted 13 November 2018; Published 27 December 2018

Guest Editor: Xihong Zhang

A brief review of experimental methods for testing blast effects on structures is presented. Methods are classified in four groups: field tests, shock tubes, pendulum systems, and new techniques (blast simulator). Description of each method is given together with overall specification of possible instruments used in each test. In today's modern era of computers which are becoming powerful tool implemented in all aspects of life and also scientific research, comparison of experimental and numerical techniques is also given. Comparison of data obtained from different experimental methods show that careful planning and execution leads to reliable results in terms of pressure, impulse, stress, and damage quantification.

1. Introduction

The blast resistance of different types of civilian and military structures against accidental explosions and terrorist attacks is an important security issue. Attacks towards vulnerable structures can cause a large number of casualties especially if total collapse occurs. Reducing vulnerability of existing and future buildings and transportation terminals is a topic of major concern for researchers in both civil and material engineering. The fields in which research is being focused are primarily blast loading predictions, material behaviour when subjected to high-rate loading, structural response to impulsive loading, and protective and retrofitting measures [1]. Structural damages caused by blast loading are the combination of both immediate effects and consecutive hazards, among which is progressive collapse. This catastrophic failure mode occurs when the initial failure of one or several key load-carrying members causes a more widespread failure of the surrounding members what leads to complete collapse of the whole structure [2]. Consequently, it is of great importance to investigate and improve the response of structures to blast loading. Compared to other construction materials, concrete is generally known to have a relatively high extreme blast resistance capacity. However, to improve resistance against extreme blast loads, some existing concrete structures require additional retrofitting [3]. To enhance the blast performance of concrete, two main procedures have been widely used. The first consists of adding steel, carbon, or polypropylene fibres as an internal reinforcement to get a fibre-reinforced concrete, and second method for reduction of damage is by protecting structure with external elements such as aluminium foam or steel sheets [4]. One of the most useful information when assessing the consequences of a blast event on a building would be the accurate evaluation of dynamic response and residual load-carrying capacity of the primary supporting members. There has been a growing trend in the engineering community to find integrated solutions for the design of infrastructures across various hazards, namely, multihazard engineering. Multihazard engineering is the search for a single design concept which can adequately fulfil the demands of multiple hazards [5]. Since protection is never an absolute concept and there is a level of high cost associated with a given damage level of protection, proper assessment tools must be employed to determine within reasonable degree of accuracy the level of vulnerability of existing and new structures. Furthermore, in blast design, one can also determine an acceptable level of damage that a structure can tolerate [6].

Blast testing in general seems to best mimic the real situation of blast action on an object. It definitely can replicate with high fidelity complex configurations and conditions that appear in a real situation and are extremely difficult if not impossible to simulate in a theoretical or a computational model. Testing naturally accounts for the real material behaviour no matter how complex they are, and for the real conditions, no matter how nonideal they look like, whether these are support conditions or connections with other elements, or poor workmanship. Testing may better simulate the behaviour of secondary systems, utilities, and buildings occupants' response to the severe vibratory response of the building to blast. However, testing has its obvious limitations such as cost, environment hazard, safety risk, length of time to achieve results, limited number of repetitions, and almost inability to perform parameters studies [7].

The paper is divided into two main parts. The first part describes the most common types of experiments simulating blast loading. With the description of each type of the experiment, tables with names of the researchers and basic information (e.g., type of structural element and its dimensions, material, generated pressure, and impulse) are given. The second part describes numerical methods of blast-loading simulations.

2. Experimental Techniques

Experimental techniques can be classified as field tests, shock tubes, blast pendulum systems, blast simulator, blast chambers, and material property tests. Each technique has its own setup and specific characteristics but all have same final goal, and that is to try to simulate blast loading as realistically as possible.

2.1. Field Tests. Practical experience related to structural response of ordinary civilian buildings subjected to different military or terror attacks was accumulated in recent years, as a consequence of different terror actions and military conflicts. The accumulated data from actual incidents and experience gained from different studies, including blast tests, can be implemented in improvement of calculation and design tools, as well as design requirements and guidelines related to design of new buildings and for retrofitting (strengthening) of existing buildings [7].

The field blast tests involve tedious preparation of test specimens, prediction of blast load, and usage of high-end instrumentation such as high-speed cameras, pressure sensors, and validation of experiments. Due to the limitations of cost and possible blast charge weight to be used for the research, the charge weight usually has to be limited to a specific maximum value [8]. Blast resistance tests are normally performed on small-scale specimens of less than 2 m in each dimension. This is because full-scale tests are expensive, complex to handle, and difficult to monitor in terms of physical parameters that characterize the blast event and the specimen response [9]. The charges used are also scaled, and their dimensions became smaller than charges that can be potentially used in the eventual attack [4].

Experimental investigation using filed test can be conducted using one of the two potential test types. These are full-scale or small-scale blast test. There are advantages and disadvantages of both types of test. Small-scale tests are usually much cheaper and can be performed more easily than full-scale tests. If blast wave propagation is considered in many cases, this may lead to reliable results due to the existence of similarity laws. To satisfy the scaling laws, the scaled tests are conducted with reduced amounts of explosives, and this is an advantage that yields smaller safety distances and enables testing at more accessible testing areas. However, considerations may entirely change when structural response involving inelastic deformations and damage are considered. This is especially pronounced in cases of reinforced or masonry buildings which have complicated nonlinear characteristics and extremely complex cracking and failure and size-dependent constructional details. Under such conditions, full-scale tests often become the preferred alternative. Full-scale tests are not easy decision because they involve considerable higher costs, larger amounts of explosives, heavier elements, installation, and overall support. One possible field test setup can be seen in Figure 3 of Schenker et al. [9] that shows typical field test setup for full-scale test, military range with large open space for free blast pressure clearing, and an array of test specimens placed on a different standoff distance with regard to explosive charge. Small-scaled field test could provide valuable information on many different parameters important for blast design (windows tests, panel tests, steel elements, reinforced concrete (RC) elements, joint elements, and protective cladding) but they cannot offer information about interaction of those elements in global response of the structure. Testing of the entire building may identify the role of its different elements in the near-collapse case when these elements may form alternative paths for load transfer and reduce the likelihood of progressive collapse of the building under consideration. These phenomena can be tested only in full-scale tests [7].

The largest portion of conducted field tests is related to the research of behaviour of concrete slabs [4, 9, 11–14]. Researchers are focused on detecting new ways for slab strengthening by using different types of materials as concrete aggregate [15], adding steel [16–21], carbon [22], and polypropylene [4, 23] fibres or using higher resistance concrete classes [24]. Experiments on columns are also conducted in the attempt to determine whether or not seismically designed bridge or building columns are capable of sustaining significant blast load before collapsing or is it necessary to conduct retrofitting [5, 25–31]. Tests are summarized in Table 1.

Field tests are usually conducted on military test sites (Figures 1 and 2) and very rarely in laboratory setting, i.e., blast chambers, except in cases of small-scale tests where small amounts of explosives are used (milligrams or grams). Main reason for this is the full size of blast pressures that would be exerted on room walls if the experiment would be conducted inside relatively small laboratory. Usually there is no adequate venting of the laboratory that would enable safe clearing of blast waves without severely damaging room and injuring its occupants. Test sites are large open spaces usually located outside main urban centres (remote locations) appropriated for various activities of military training, among

Table 1: Field tests.

Author	Year	Element type	Material	Scale/dimensions (m)	Charge type	Charge weight (kg)	Standoff distance (m)
Đuranović [11]	2002	Slabs	RC	1 : 4 and 1 : 10	PE4	0.078	0.1–0.5
Rodriguez-Nikl [25]	2006	Columns	RC and RC + ACJ	1 : 1	AFNO	558	4.36
Ohtsu et al. [23]	2007	Slabs	RC, PPFRC, PVAFRC, and PEFRC	0.6 × 0.6	SEP	10	Contact
Wei et al. [12]	2007	Slabs	RC	1.22 × 1.22	TNT	1.16 and 1.71	Contact
Fujikura et al. [26]	2008	Columns	RC and CFST	1 : 4	N/A	N/A	N/A
Fujikura and Bruneau [27]	2008	Columns	RC and RC+SJ	1 : 4	N/A	N/A	N/A
Schenker et al. [9]	2008	Slabs	RC and FRC	1 : 1	TNT	1000	20
Davis et al. [28]	2009	Columns	RC	1 : 2	AFNO	N/A	N/A
Wu et al. [16]	2009	Slabs	NC, UHPFC, RUHPFC, and EBFRP	2 × 1	Comp B	1–20	0.75–3
Williamson et al. [29]	2010	Columns	RC	1 : 2	AFNO	N/A	N/A
Fujikura and Bruneau [5]	2010	Columns	RC and RC+SJ	1 : 4	N/A	N/A	N/A
Yusof et al. [8]	2010	Panels	RC and SFRC	0.6 × 0.6	N/A	1	0.6
Fujikura and Bruneau [30]	2011	Columns	RC and CFST	1 : 4	N/A	N/A	N/A
Wang et al. [13]	2012	Slabs	RC	1 : 1, 1 : 1.25 and 1 : 1.67	TNT	0.19–0.94	0.3, 0.4 and 0.5
Foglar and Kovar [17]	2013	Slabs	RC and FRC	6 × 1.5	TNT	25	15–30
Tabatabaei et al. [22]	2013	Panels	RC and LCFRC	1.83 × 1.83	AFNO	38.5	1.065, 1.37 and 1.675
Yankelevsky et al. [7]	2013	Buildings	RC	1 : 1	N/A	N/A	N/A
Zhao and Chen [14]	2013	Slabs	RC	1 × 1	TNT	0.2, 0.31 and 0.46	0.4
Castedo et al. [4]	2015	Slabs	RC, RC+SS, SFRC, and PPFRC	1 : 1	PG2, RDX	2 and 15	1 and 0.5
Foglar et al. [18]	2015	Panels	RC and FRC	6 × 1.5	TNT	25	0.45
Li et al. [24]	2015	Slabs	NSC and UHPC	2 × 1	N/A	1 kg	Contact
Mao et al. [19]	2015	Slabs	UHPFRC	0.6 × 0.6	PE4	0.21	0.5
Mazurkiewicz et al. [31]	2015	Columns	HKS-300	1 : 1	HE	4	0.5
Alengaram et al. [15]	2016	Slabs	NC, OPSC, OPSFRC	2 × 1	TNT	1, 5 and 10	1.5
Codina et al. [32]	2016	Columns	RC	1 : 1	Gelamon VF65	12.3	0.6 and 1
Xu et al. [33]	2016	Columns	UHPFRC and HSRC	1 : 1	Emulsion exp.	1.4–48	1.5
Wu and Li [20]	2017	Slabs	RC and RC+ALFC	2 × 0.8	TNT	6, 8 and 12	1.5

RC: reinforced concrete, NC: normal concrete, OPSC: oil palm shell concrete, OPSFRC: oil palm shell fibre-reinforced concrete, SS: steel sheet, SFRC: steel fibre-reinforced concrete, PPFRC: polypropylene fibre-reinforced concrete, FRC: fibre-reinforced concrete, CFST: concrete-filled steel tube, RC + SJ: reinforced concrete with steel jacket, NSC: normal strength concrete, UHPC: ultrahigh-performance concrete, HKS-300-steel I-shaped cross section, PVAFRC: polyvinyl alcoholic fibre-reinforced concrete, PEFRC: polyethylene fibre-reinforced concrete, PPFRC: polypropylene fibre-reinforced concrete, RC+ACJ: reinforced concrete with advanced composite jackets, LCFRC: long carbon fibre-reinforced concrete, UHPFC: ultrahigh-performance fibre concrete, RUHPFC: reinforced ultrahigh-performance fibre concrete, EBFRP: externally bonded fibre-reinforced polymer plates, RC+ALFC: reinforced concrete with aluminium foam claddings, UHPFRC: ultrahigh-performance fibre-reinforced concrete, and HSRC: high-strength-reinforced concrete.

which is also training with explosive charges. Specialized personnel, trained for explosive handling and detonation, usually conduct experiments. Danger of personnel injury reduces to minimum because operators and researchers are securely located in protective structures, concrete bunkers, during the detonation of explosive charge. Depending on the needs of researchers, various instruments can be planned for data acquisition. Detailed descriptions of various instruments used can be found in Section 2.5. Depending on the tested element, supporting structure is usually constructed in order to provide desired boundary condition. If columns are tested, besides massive foundations that simulate fixed bearings, additional steel [5, 29] structure is constructed for simulating column top/head boundary condition. This additional structure is also used for mounting extra mass on the top of the column to simulate mass of the bridge superstructure, if bridge columns or mass of the upper building storeys are tested or if columns from public or residential buildings are tested. Possible setting for column testing is also to lay columns flat with the ground [32] or to bury the column [33]. Columns are buried in such a way that one of the faces is exposed to the blast pressure. This reduces the influence of clearing, additional pressure wave refraction, and reflection. In this setting, adequate standoff distance is provided with

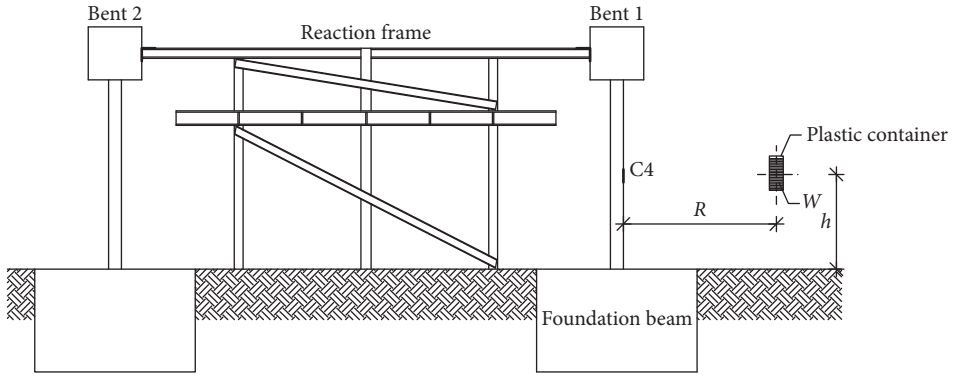

W: explosive charge weight
h: charge height
R: standoff distance

Figure 1: Test setup for column testing [5].

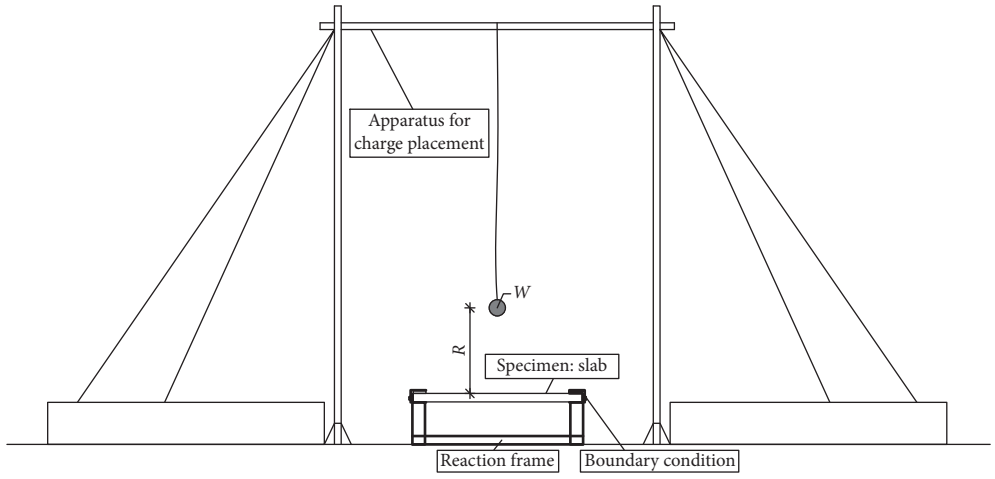

W: explosive charge weight
R: standoff distance

Figure 2: Test setup for RC slab testing [16].

hanging or placing desired charge on the top of the styrofoam sheets. In buried settings, hydraulic jacks are usually used for providing additional level of axial force in the column [33]. Similar setup for charge placement is used in field-testing of slabs. Slabs are field tested utilizing steel reaction table [16] or trench [18], which can be dug in the earth and slab is then laid on top of it. Either of these setups is designed to provide clear space beneath the test specimen in order to enable free deformation. Steel reaction table beams can be designed to provide different boundary conditions on one, two, three, or all four edges/sides of the slab.

There is no universal test setup for field blast tests, especially if different types of construction elements are considered. Test setup depends on the specific requirements of the researcher, scale, type, and shape of the specimen and information which is needed from the experiment (if instrumentation is needed or not). Careful planning is essential to maximize test efficiency and minimize costs and safety concerns.

2.2. Shock Tubes. Shock tubes have been proven to be a most versatile and resilient tool for the investigation of shock-wave-related problems under a laboratory condition covering a wide variety of fields both in fundamental science and in applied technology. Tubes are used for analysis of the physical and chemical processes generating one-dimensional, nondissipative flows [34–36]. They can be divided into large, medium, small, and microscale based on length and inner diameter of the tube [37]. Generally, the shock tube consists of two major sections, a driver section and an expansion section. Blast pressures are generated when a rupture diaphragm, placed between the two sections, fails due to pressure in the driver section. A shock wave then travels down the expansion section and loads the test specimen at the end of the expansion section. In some cases, the driver could be baffled to reduce the effects of reloading by smaller reflections that exist in the shock tube. Due to the construction and the functional principle of the shock tube, the structural element located at the end of the tube can be

loaded with a precisely defined pressure-time history. It is adjustable by the initial pressure and the length of the high-pressure section of the shock tube. The resulting planar blast wave is exerted on the test specimen evenly and normal to the element surface [38–41]. For larger test specimens the shock tube can be fitted with an additional expansion section making it possible to test larger structural systems [42]. If nonplanar specimens such as columns or beams are tested, a load transfer device, which consists of steel metal sheets connected to a series of steel beams, could be used. This additional apparatus is used to transfer shock-wave pressure as a uniformly distributed load along the compression face of the specimen. Table 2 gives a list of conducted shock tube experiments on construction elements.

The test gas flow between the shock wave and the interface has a very short duration, and it can be disturbed by the various wave systems that propagate in the tube because of its limited dimensions. The most significant effects concern the perturbations related to the presence of the wall boundary layer and noninstantaneous rupture (opening) of the diaphragm (and combined effects). However, if these effects are taken into account, it is possible to optimise parameters of interest independently of the disturbing phenomena [34].

There are several possibilities for improving the performance of shock tubes. Some of them are area reduction close to the diaphragm, use of double-diaphragm tube, combustion tube, and/or free piston tube. If area close to the diaphragm is reduced, there is a quasistationary expansion of driver gas in the area transition zone, which increases the efficiency of the thrust and consequently Mach number. Additional third section added to the double-diaphragm tube that is used as a test section. Expanded gas from the second chamber is used as a driver gas for the test gas in the third chamber what, again, consequently increases the Mach number and reduces the test time. Combustion tube is used to produce the increase in the sound of speed by temperature increase. The problem here is to obtain uniform combustion without detonation, and this is usually realized by arranging significant number of spark plugs in spiral along the high-pressure chamber. Increase in the Mach number is partly compensated by strong deceleration of the shock wave due to sharp pressure fall after the combustion. Free piston tube is used for fast compression of a light gas used as a driver. This compression carried out by a piston launched at high speed in a tube is serving as a compression chamber after which compressed hot gas ruptures the diaphragm. This is the most efficient process to create a shock wave of high intensity [34].

The BakerRisk test site in San Antonio [42] has a 0.75 m^2 (8 ft^2) target area in its normal configuration and can be configured to deliver a variety of blast pressure and impulse combinations with maximum possible peak pressure of 3 bar (45 psi) with a maximum impulse greater than 660 bar·ms (1000 psi ms). Shock tubes of similar construction and capability are blast load simulator (BLS) which are situated at the U.S. Army Corp of Engineers (USACE) Engineer Research and Development Centre (ERDC) in Vicksburg, Massachusetts, USA [10], at the University of Ottawa Blast Research Laboratory, Canada [46, 50], at the testing ground of Swedish Defence Research Agency (FOI) in Marsta, Sweden [44], and at the Ernst-Mach-Institute in Freiburg, Germany [39]. Listed tubes are slightly different by their internal cross section near the test area and pressure levels exerted on test specimens but their work mode is very similar. A wide range of measurements are possible during shock tube testing; dynamic measurements, dynamic load measurements, strain measurements, high-speed camera video, normal video, and still photography capabilities are available depending on shock tube setup and researcher requirements. A high-speed camera is used for recording the dynamic response of tested specimens. Usually the high-speed camera is mounted outside the shock tube and is oriented to record the motion of the specimen. If positioned perpendicular to the shock tube, it can record deflections and velocities which are determined from sequential images taken during testing [10, 38, 43, 46, 48, 49, 51]. Propagation of the damage pattern can also be analysed if the camera is placed in such a way to have a clear view of the specimen surface of interest. The schematic layout of the shock tube is presented in Figure 3, and the photography of the field-installed BakerRisk shock tube can be seen in Figure 8 of Schleyer et al. [42].

2.3. Blast Pendulum Systems. Blast measurements for experimental testing of smaller structural parts could be conducted using pendulum systems situated in blast chambers. Typically, a four-cable ballistic pendulum system is employed to measure the impulse imparted onto the front face of the specific specimen. The recorded pendulum swing gives a direct indication of the height reached by the pendulum and hence the maximum potential energy of the system after the dissipation of the energy in plastic work. The value of this maximum potential energy can be used to calculate the maximum velocity of the whole pendulum system as it swings back through its initial zero position. The linear momentum (mass times velocity) associated with the whole pendulum mass at this point must be equal to the initial impulse applied to the beam, as long as mass has been constant, and no other forces have been applied. In this way, the pendulum swing gives an accurate measure of the applied impulse [52–55]. The balance weight is adjusted before each test to ensure that the centre of the mass of the whole pendulum system is close to the centre point between the two pairs of the cables. TNT charge is used to produce impulsive loading on the front face of the specimen which pushes the pendulum to translate. Based on the oscillation amplitude recorded by oscilloscope, the impulse exerted onto the pendulum can be calculated. Besides oscilloscope, laser displacement transducers could be used for translation measurements. The front of the pendulum consists of the steel frame onto which the specimen is clamped [56–58]. Typical experimental setup for blast experimentation using ballistic pendulum system can be seen in Figure 1 in [56]. Figure 4 depicts the schematic view of the pendulum system. Charge weights in the pendulum blast test range from 3 to 50 g if experiments are conducted inside the blast chamber,

Table 2: Shock tube experiments.

Author	Year	Element type	Material type	Scale/dimensions (mm)	Shock wave (kPa)	Impulse (kPa ∗ ms)	Load transfer
Toutlemonde et al. [43]	1993	Slabs	RC	φ 900	1700	N/A	PW
Schleyer et al. [42]	2007	Panels	STS	1 : 4	38–221	2013–4358	PW
Magnusson et al. [44]	2010	Beams	NSC and HSC	1 : 1	1200–3200	6300–11130	PW
Ellis et al. [10]	2014	Panels	UHPC	1626, 864 and 51	N/A	810–2050	PW
Stolz et al. [38]	2014	Slabs	DUCON	2410 × 1140	35–250	N/A	PW
Zhang et al. [45]	2014	Plates	Steel 1008 and 1018	50.8 × 203.3	375	N/A	PW
Aoude et al. [46]	2015	Columns	UHPFRC (CRC)	1 : 1	12.6–108.6	109–964	LTD
Thiagarajan et al. [40]	2015	Slabs	HSC-VR, HSC-NR, NSC-VR and NSC-NR	1 : 3	350–390	6790–7710	PW
Haris et al. [41]	2017	Panels	Polyurea, STF, foam, and STF-infused foam	120 × 110	186	N/A	PW
Lee et al. [47]	2018	Beams	SFRC	125 × 250 × 2438	22.78–67.81	196.02–680.4	LTD
Lacroix and Doudak [48]	2018	Beams	24F-ES Spruce Pine glulam + FRP	137 × 222 × 2235	41.2–76.2	419.1–1110	LTD
Poulin et al. [49]	2018	Panels	CLT SPF	105 (175) × 445 x 2500	5.8–58.6	59.4–690.7	LTD

UHPFRC: ultrahigh-performance fibre-reinforced concrete, CRC: compact reinforced concrete. UHPC: ultrahigh-performance concrete, STF: shear thickening fluid, NSC: normal strength concrete. HSC: high-strength concrete, STS: stainless steel, DUCON: ductile concrete, VR: high-strength low alloy vanadium reinforcement, NR: normal reinforcement, SFRC: steel fibre-reinforced concrete, FRP: fibre-reinforced polymer, CLT SPF: cross-laminated timber with Spruce pine fir, PW: pressure wave, and LTD: load transfer device.

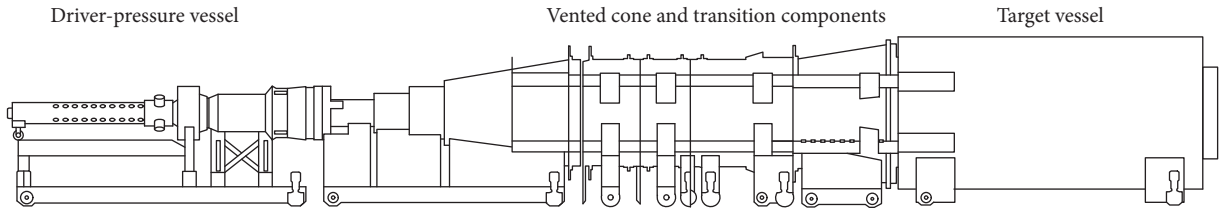

Figure 3: Schematic representation of Vicksburg BLS [10].

but there are versions of pendulum systems which are adapted for larger weight sizes [59], up to 2500 g, and are installed in open spaces (Figure 5). Specimens vary in shape and size depending on research requirements. The most common shape of specimens for blast pendulum tests is rectangular with dimensions from 76 mm up to 400 mm (700 mm if exterior blast pendulum system is considered), but even circular or even small-scale beams can be tested. Table 3 gives summary of blast pendulum tests.

Pendulum systems are used for small-scale blast experiments in laboratory setup. They are used for investigation of local effects of blast loads and have a wide spectrum of experimental possibilities. Pendulum tests were conducted on metal [56, 63, 65], glass [51], and composite panels [57, 60–62, 64]. Panels were tested for structural response on blast load in order to determine possibilities of their use for structural strengthening.

2.4. Blast Simulator. Field experiments, although generally effective, are often expensive, dangerous, and in many cases do not provide clear visual evidence and quantitative data of structural response throughout the blast event. In order to provide blast-like loadings on structures in a controlled laboratory setting, the blast simulator was designed and constructed (University of California, San Diego, USA, 2006.). The blast simulator is a ultrafast, hydraulically driven, computer-controlled impulse generator. It is designed to produce an impulse by impacting the specimen with a mass in a controlled manner. In this way, the simulator can produce quantitative and qualitative, high resolution data and what is most important is it ensures repeatability of experiments eliminating blast wave and fireball interference with measuring instruments. The simulator generates impulses using ultrafast, computer-controlled hydraulic actuators with a combined hydraulic/high-pressure nitrogen energy source called blast generators (Figure 6). The actuators are used in conjunction with appropriate loading media, which attached to the variable masses assist in the appropriate loading conditions for various blast loads. Detailed description of the blast simulator inner workings can be found in [67–69]. Blast simulator construction and actuator configuration can be seen in Figure 1 in [69].

Tests are conducted using one of the two methods selected based on the test requirements. The procedure for determining force-time history and impulses is dependent on the type of experiment. The first method involves an unattached mass, and the second involves an attached mass. For the unattached configuration, a thin plate is attached to the piston rod, and it pushes the impact mass towards the specimen. At a specified time, the rod is retracted, letting the impact mass travel forwards and impact the specimen. The second, more common, test type is the attached test. In this

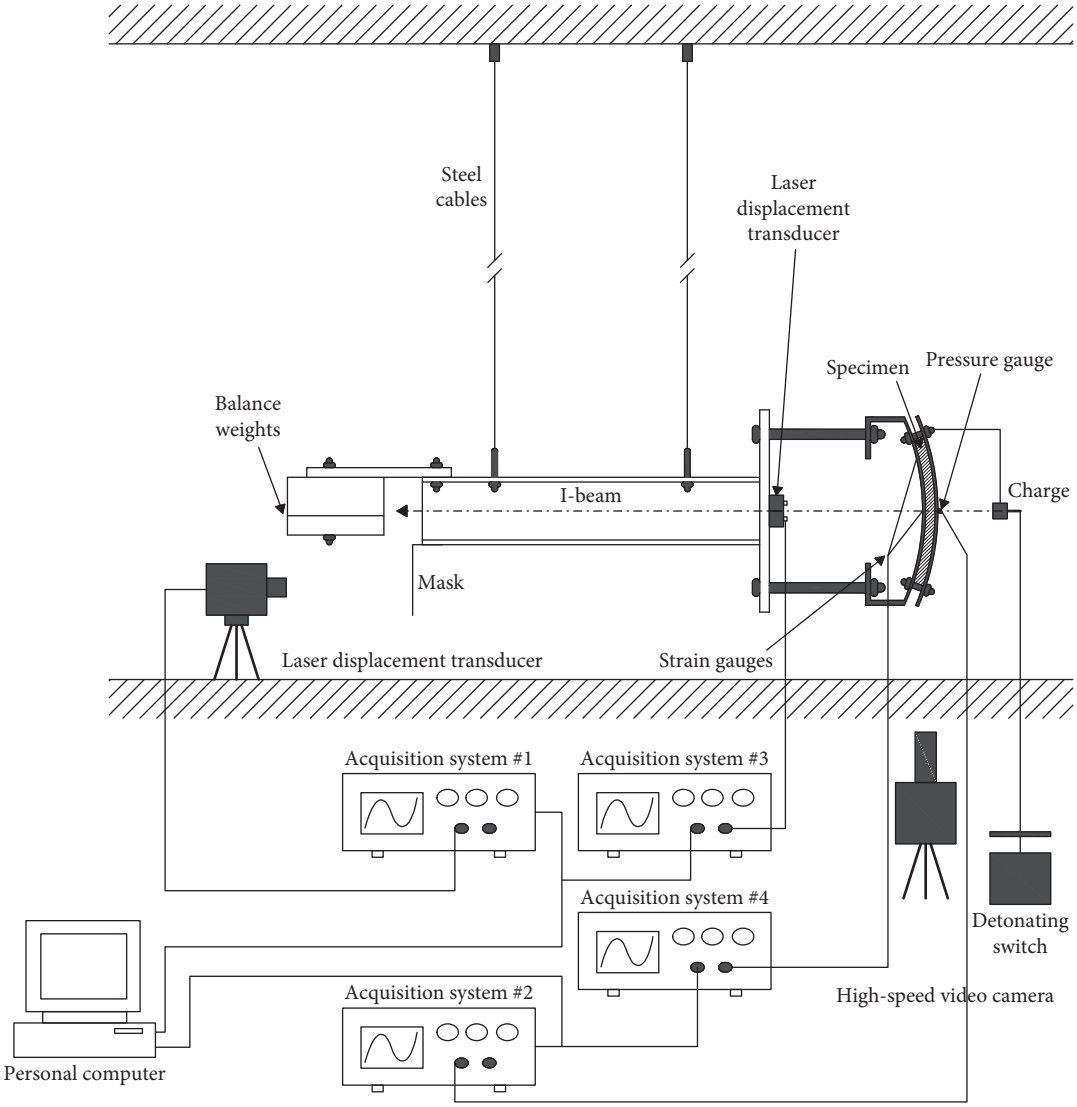

Figure 4: Ballistic pendulum experimental setup [57].

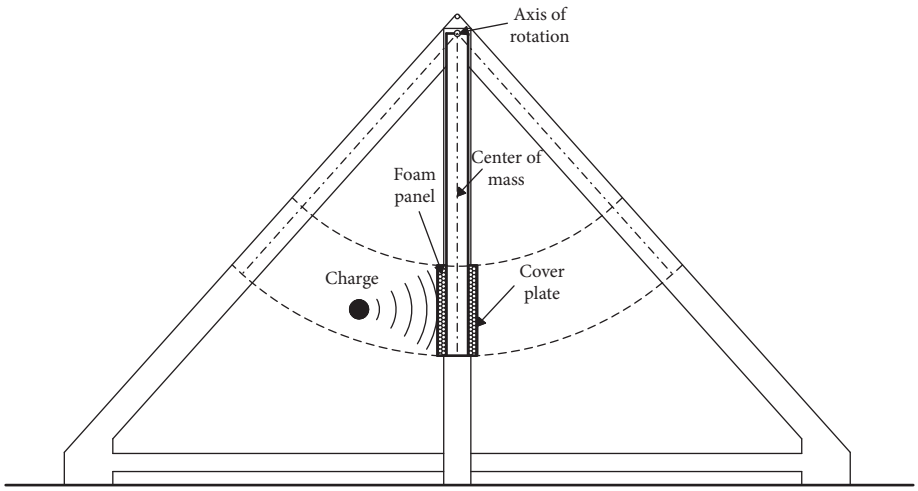

Figure 5: Field blast pendulum system [59].

Table 3: Blast pendulum tests.

Author	Year	Element type	Material type	Dimensions (mm)	Charge type	Charge weight (g)	Standoff distance (mm)	Impulse (ns)
Humphreys [52]	1965	Beams	Steel	N/A	DuPont EL-506-D	N/A	N/A	N/A
Jones et al. [53]	1970	Plated	Mild steel and aluminium	76 × 129	DuPont	N/A	N/A	N/A
Jones et al. [54]	1971	Beams and plates	Mild steel and aluminium	128 (× 128)	DuPont	N/A	N/A	N/A
Hanssen et al. [59]	2002	Panels	Aluminium foam	684 × 700	PE4	1000–2500	500	364.7–1305.3
Langdon et al. [60]	2009	Panels	GLARE	200 × 200	PE4	4–14	13	11–32
Shen et al. [57]	2010	Panels	Al-5005 H34 sheets and ALPORAS foam	400 × 400	TNT	20–60	250 and 350	15.8–41.2
Fallah et al. [61]	2014	Plates	Dyneema	300 × 300	PE4	12–50	50	17.7–114.4
Guan et al. [62]	2014	Panels	Divinycell H	Φ 90	PE4	3–7	90	5.89–11.08
Henchie et al. [63]	2014	Plates	Domex-700 MC steel	Φ 106	PE4	5–40	150	10.4–63.98
Jing et al. [64]	2014	Sandwich shell	Aluminium sheets and foam	250 × 250	TNT	10–40	100	8.73–44.38
Li et al. [65]	2014	Sandwich panels	Aluminium AL-1200H18	250 × 250	TNT	10–30	100–240	11.8–26.7
Langdon et al. [56]	2015	Plates	Mild steel, Armox 370T, AL-5083H116, and GFPP	300 × 300, 400 × 400	PE4	7–50	25 and 38	13–116.8
Ghoor [66]	2018	Panels	FRPMS and LCP	400 × 400	PE4	10–25	100	17.32–35.6
McDonald [58]	2018	Plates	RHA, IRHA, HHA, and ARS	400 × 400	PE4	30–75	50	61.2–127.9

Dyneema: ultrahigh molecular weight polyethylene fibre composite, Divinycell H: crosslined PVC foam, GLARE: fibre metal laminate, GFPP: glass fibre-reinforced polypropylene, RHA: rolled homogeneous armour, IRHA: improved rolled homogeneous armour, HHA: high hardness armour, ARS: abrasive resistant steel, FRP+MS: fibre-reinforced polymer moulded sandwich (Airex C70:75 core), and LCP: laminated composite panels.

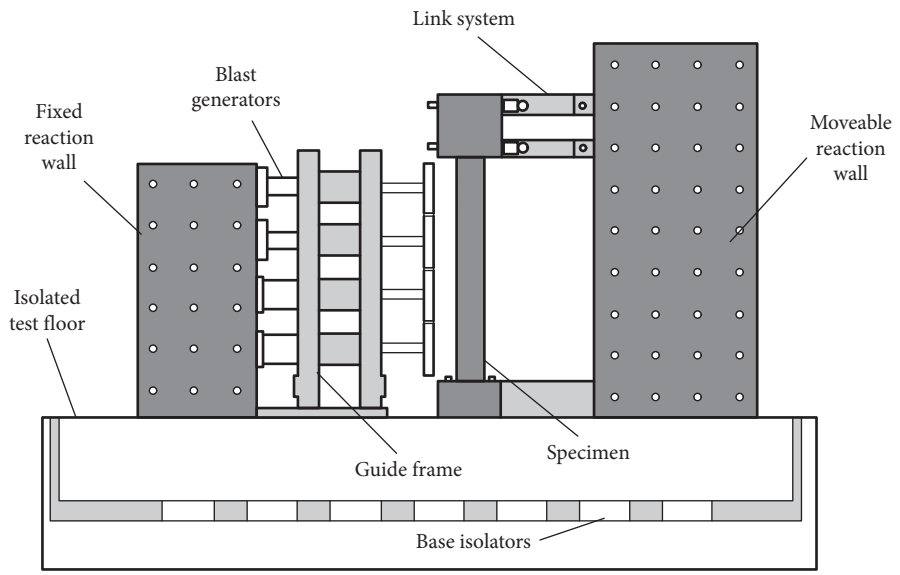

Figure 6: Blast simulator site scheme [67].

type of test, the hydraulics is connected to the impact mass throughout the collision. At a specified time, the hydraulics begins to pull back on the impact mass near the end of the collision. This pulling back prevents a double-hit and tailors the impact so that the loading is blast-like in duration and shape [67]. The simulator can be applied to a wide range of interesting problems which include the development of novel hardening strategies [71] and the simulation of complex loading environments [72, 73]. The blast simulator is not limited to producing just external blast loads, but can generate

a multitude of high-rate loading effects, such as shock loads of components and confined explosions. Comparing the data from blast simulator tests to computer simulations as well as a field tests using explosive charges, the experimental blast simulator impulse was verified. It was confirmed that short duration impulsive loading can be achieved from structures with planar geometry [67–69]. Table 4 gives a list of test performed using the blast simulator.

Data comparison shows very good overlap of measured and simulated values based on which it can be concluded that the blast simulator can provide realistic blast results. Measured and numerically simulated displacements from concrete wall subjected to blast load can be seen in Figure 10 in [67]. Oesterle in 2009 tested thirty specimens of different types of concrete walls at Blast Simulator Facility. These tests included reinforced concrete walls, unreinforced and reinforced concrete masonry unit walls, and same wall types retrofitted with carbon fibres and polyurea [75, 76]. Comparison of steel column displacements measured from the blast simulator and field tests can be seen in Figure 14 in [67]. Steel columns were tested to simulate vehicle-borne explosives of 454 kg (1000 lbs) to 680 kg (1500 kg) located at the curb side. Such blast scenarios generated a nonuniform load along the height of the column with a higher impulse at the base and a decreasing impulse along the height of the column. This required precise configuration of the valve commands and the initial position of the piston rod in order to ensure a synchronized impact. Comparison of results showed that the simulator is effective in producing loads which can capture the maximum displacement and overall response of the column when scaled distance is equal or above two. However, the blast simulator cannot generate blast load with sufficient accuracy due to temperature effects and other parameters because of the close proximity of the charge and subsequent fireball when the scaled distance is smaller than two [77–79].

2.5. Blast Chambers. Blast chambers are structures used to fully or partially contain the effects of high explosions. They are produced for a number of different uses: for the research of different aspects of explosive loading and explosive characteristics, for development purposes of different types of materials or construction elements, as well as for destruction of munition. Based on the intended purpose, the chamber is designed accordingly. The chamber intended to withstand multiple detonations without sustaining any damage is designed considering liner-elastic response, while chambers intended for one-time extreme event is designed considering plastic response. Majority of blast chambers are intended for multiple use and can sustain 20% to 27% larger charge weights in comparison with the designed value [80]. At this charge weight level, first detectable plastic strains can be detected in the chamber. Usually chambers are designed to sustain detonation of up to 1 kg of explosive charge. Basic geometry of blast chambers is either spherical or cylindrical, but if spatial or operational requirements dictate, a rectangular geometry can also be designed to contain internal detonation. Charge is usually detonated in the centre of the spherical chamber, while charge can be placed optionally in the rectangular chamber. Characteristic of blast chamber is that the tested element as well as chamber walls is loaded with multiple pressure spikes as a result of pressure reflection from chamber walls resulting in nonuniform load at different locations inside the chamber. Chambers usually have places intended for instrumentation placement for recording pressures inside the chamber. These instruments are side-on and face-on pressure sensors, and if partially confined chambers are considered, high-speed cameras can be installed to monitor blast door opening and pressure wave expansion. Table 5 gives list of conducted research in blast chambers.

Research is conducted on small-scale specimens, usually slabs [82, 83], but there is several research about strain growth in chamber walls [70, 81, 84] and shock wave expansion and reflection inside the chamber [85] Examples of blast chambers used in experiments can be seen in Figures 7 and 8.

2.6. Material Property Tests. Dynamic behaviour of materials is strain-rate dependent. If compared to statically determined properties, increase in strength strain capacity and fracture energy is observed. This increase is taken into account by using dynamic increase factor (DIF). There are several possible methods to determine dynamic properties of materials as the Charpy pendulum, drop-weight impact, plate impact, servo-hydraulic test machine, Split-Hopkinson pressure bar (SHPB), gas gun, and explosive field tests [87, 88]. Most commonly used test is SHPB (Figure 9) but all depends on the availability of certain method to researcher. In Charpy pendulum test, the specimen (usually thick beam) is impacted by swinging pendulum directly opposite the notch which is machined in the middle of the specimen supported in a horizontal plane. The test can be easily instrumented, and information about energy dissipation or strains can be recorded during impact test. Drop-weight test (plate impact) consists of a known weight dropping from a predetermined height to the test specimen supported in the horizontal plane. Impact speed can be determined using equations of motion or by optical sensors located in the vicinity of the test specimen. Advantage of this type of test is a wider range of test specimen geometries. High-strain-rate testing of various specimens can be conducted using servo-hydraulic testing machines. Specimens can be loaded with pulsating or alternating loads using periodic or random signals. There is a wide range of force capacity of these machines (5 kN to 2500 kN) with different grip types depending on intended use, flat for compression testing, or clamping for tensile testing. Usually machine has an integrated force and displacement sensor for recording information during testing. Hopkinson bar technique can be employed for determination of different material properties. There are several types of Hopkins bar tests, the punch-loaded Hopkinson bar, the compression bar, the tensile bar, and the Hopkinson bar shear test. Main principle for this test is to bind specimen into the inertia bar and the input bar which is then loaded through the weight bar accelerated using gas projectiles. The specimen should have an adequate interface with

Table 4: Blast simulator tests.

Author	Year	Element type	Material type	Dimensions (m)	Impact velocity (m/s)	Pressure (MPa)	Impulse (MPa ∗ ms)
Gram et al. [74]	2006	Columns	RC	0.36 × 0.36 × 3.28	1.5–30	N/A	15.8
Oesterle [75]	2009	Walls	CMU and CMU + CFRP (RC + frangible panels)	0.268 × 0.146 0.350 × 0.122	4–8 (5–23)	N/A	0.7–1.9 (1.9–5.9)
Oesterle et al. [76]	2009	Walls	CMU and CMU + CFRP	2.68 × 1.46	4–8	1.55	1.1–2.0
Stewart [77]	2010	Columns	A992 Gr. 50 steel	0.25 × 0.25 × 3.32 0.37 × 0.37 × 3.32	4–45	1.1–131.3 (233.3)	2.4–55.6 (53.1)
Huson et al. [73]	2011	Water bladder	XR-5 polyester and U1940 nylon	0.41 × 0.41	10–25	0.5–1	0.62–16.2
Rodriguez-Nikl et al. [68]	2011	Columns	RC and RC CFRP	N/A	N/A	10	6.8–16.9
Huson [72]	2012	Joints	CFRP and balsa	0.60 × 1.22 × 1.22	10–25	3.1–10.34	6.9–34.5
Li et al. [50]	2012	Columns	RC LS and RC NS	0.26 × 0.26 × 2.4	10–25	N/A	5.3–15.9
Stewart [78]	2012	Columns	A992 Gr. 50 steel	0.37 × 0. 37 × 3.32 (S and W)	13–45 22–65	N/A	15 ()–53.8 (39.4–107.4)
Freidenberg [69]	2014	Wall	Sure-board	3.7 × 1.3	10	3200	4
Stewart et al. [67]	2014	Columns	A992 Gr. 50 steel	0.25 × 0.25 × 3.32 0.37 × 0.37 × 3.32	4–45	1.1–131.3 (233.3)	2.4–55.6 (53.1)

Sure-Board: C-shaped studs of high-strength low alloy vanadium steel with cement-board and gypsum-board panel. UCSD: University of California, San Diego. CFRP: carbon fibre-reinforced polymer. RC LS: reinforced concrete limited seismic. RC NS: reinforced concrete nonseismic. S: strong axis. W: weak axis.

Table 5: Blast chamber tests.

Author	Year	Element type	Material type	Scale or dimensions (m)	Charge type	Charge weight (g)	Standoff distance (m)	Pressure (kPa)	Impulse (kPa ∗ ms)
Whenhui et al. [81]	1997	Chamber wall	Steel	0.852 × Φ 0.425	RDX	9.1, 18.2 and 27.4	0.212	N/A	N/A
Wu et al. [82]	2007	Slabs	RC and RC NSM CFRP	1.3 × 1.0	Pentolite and comp B	60 and 2000	0.6	N/A	N/A
Wu et al. [83]	2009	Slabs	RC and RC NSM CFRP	1.3 × 1.0	Comp B	2000	0.6	N/A	N/A
Wu et al. [70]	2013	Chamber wall	N/A	1 : 1	PE4	95–200	1.3 and 1.5	250–1100	50–225
Snyman et al. [84]	2016	Blast chamber	MS and MS nylon	1:5 (1.2 × Φ 1.0)	Comp B	24 and 40	0.5	4129 (476)	312–597
Jiba et al. [85]	2018	Shock wave	Fine water mist	1.2 × Φ 1.0	PE4	20	0.5	N/A	N/A

NSM CRFP: near-surface-mounted carbon fibre-reinforced polymer. MS: mild steel.

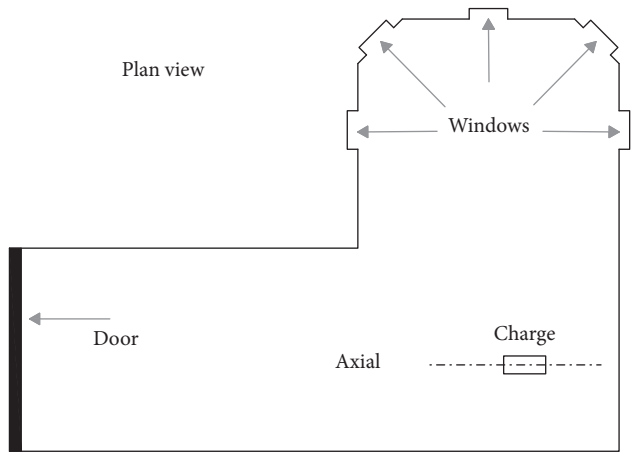

Figure 7: Rectangular blast chamber [70].

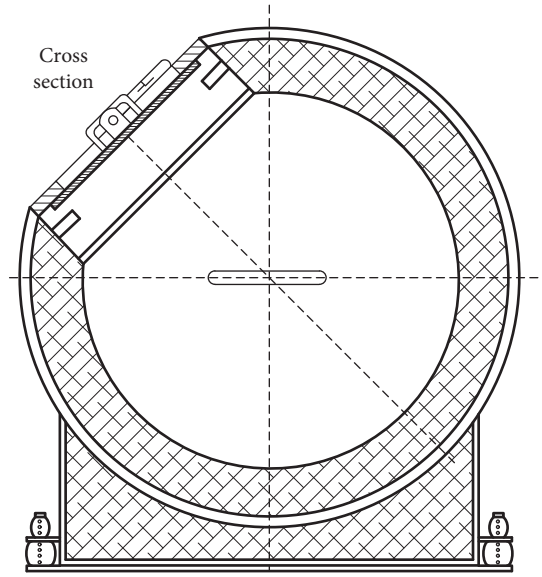

Figure 8: Spherical blast chamber.

bars in order to avoid shear failure within grip and the specimen and to avoid stress concentration. Strain gauges on input and inertia bar record incident and reflected stress waves. Impact testing of materials can also be conducted using a high-pressure gas gun. Projectile is accelerated down the barrel by gas that is fled to a chamber. Gas is restrained by a plastic diaphragm, and when the predetermined pressure value is achieved, diaphragm is burst to produce acceleration of projectile. A gun barrel is usually instrumented and can capture force-displacement histories for further analysis.

2.7. Instrumentation. Measuring of blast loads on structures is a complex task. Instruments should be placed in such a way that they do not interfere with the load distribution on the surface of the observed element and to avoid their damage and/or destruction when subjected to blast wave. The properties of blast waves as they strike the structure are most commonly recorded in terms of pressure, and the design and use of pressure gauges suitable for recording the history of blast wave pressure is an important aspect of structural loading research [90]. The damage potential of a blast wave is associated with both the force it exerts on an object and the duration over which the force is applied. An assessment of this damage potential requires measurements of the peak static overpressure and the total impulse per unit area of the blast wave. During blast measurements there are several undesired environmental influences which can severely distort the signal output. Influences include high temperatures, ground shocks and their associated strain waves, intense light, fragment impact, ionized gases which coupled with submicrosecond pressure-time rise and extremely high-frequency response from the measuring transducers and signal conditioning make blast measurements an extremely challenging task [91, 92]. Broad spectrum of various instruments is used in blast measurements depending on required data for analysis. From conventional instruments linear variable differential transformer (LVDT), both mechanical and laser, are used for deformation measurements, different types of accelerometers used for measuring test specimen acceleration after blast wave impact (specimen velocity and deformation can be determined in postblast analysis) and strain gauges, typically for measuring strains on reinforcement in reinforced concrete specimens or on steel plates. These instruments are usually mounted on opposite side of test specimen in relation to blast wave incidence in order to provide protection against damage or destruction. Mentioned instruments are usual in static experimental setups while in dynamic they are required to have greater acquisition speeds in order to capture high strain rates produced by dynamic loading. Mentioned instruments are used for measuring secondary blast effects; deformations, accelerations and strains of tested specimens but not for primary detonation products; blast incident and reflected pressure, impulses and blast duration. First attempts to develop blast pressure transducers to measure static overpressure was made by U.S. and British laboratories in 1950s and 1960s in order to measure pressures originated from atmospheric nuclear testing [91]. Two types of pressure transducers were researched: pencil and lollipop probes. Lollipop probes were in time abandoned, and nowadays pressure transducers for measuring blast pressures at locations above ground level are mainly pencil probes. In addition to transducers for measuring free air blast pressures there are transducers for measuring reflected pressures, ground-surface transducers. Pencil probes and ground-surface transducers are very different in their design [91, 93].

2.7.1. Pencil Probe. Pencil probes are side-on transducers that record free field pressures at varying distances from blast source. Their design must minimize interference with the flow behind the shock front (Figure 10). Blast wave will become distorted at its higher frequencies when

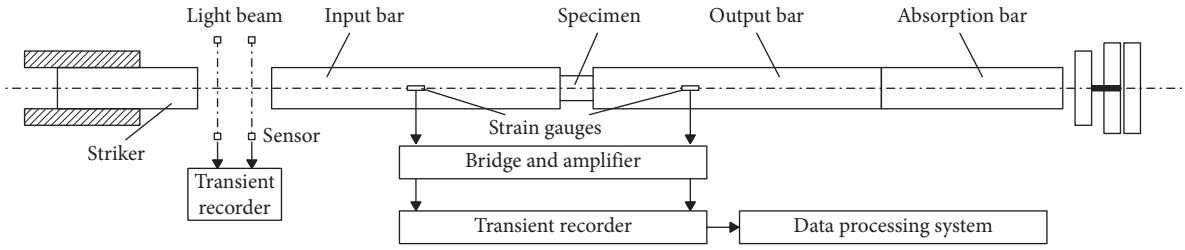

Figure 9: Schematic representation of an SHPB setup [89].

encountering the probe tip, but it will reconstitute itself by the time it arrives at the sensing face that is located transverse to the longitudinal axis of the probe. The probe is tapered over its first 5 cm of length and then widens into a cylindrical body with a flat sensing surface on one side [94, 95]. Probes tip should be pointed to an incident, planar blast wave in order to permit accurate measurement of it static overpressure preventing wave reflection and amplification. From the first appearance of the probe, there was little change in its design. Significant changes include replacement of probe material from ceramic to quartz and ICP® electronics (registered brand of PCB Piezoelectronics Corporation) were integrated enabling 5 V full-scale output for each of its various pressure ranges [91, 93]. Probe axis should be aligned incident to the incoming air blast wave in order to avoid errors of the measurement. Proper placement of pencil probe can be seen on Figure 3 in Walter [91]. Field test have shown that the maximum misalignment of probe axis should be within $\pm 5^{\circ}$ in order to conduct accurate measurements [96].

Both mechanical and electrical isolation should be provided. Transducer is mechanically adapted to an electrically conductive test stand or holder by a nonconductive material because it provides electrical isolation between the probes case and the path for any electrical grounding through the stand. Probes placed on hard surfaces are susceptible to blast ground shocks that could disturb the measurements but this problem is solved by placing the probe stand on low-density foam that would block this transmission path. Exposure to high temperatures can also result in an error in measurements; it can cause false negative pressure that is occurring due to a thermal expansion in the internal housing of the transducer. The expansion results in a slight release of the preload on the stacked quartz elements. This problem is resolved with a tight wrap of black electrical tape around the sensor [91, 97, 98].

Transducer placement is dependent on the test configuration and quantity of the explosive test items, on other items located in the test area, on the height of the test specimen and explosive at detonation, on preparation of the ground surface, etc. One possible field sensor setup can be seen in Walter [99] It is desired to have the sensors located in the Mach stem what enables the easiest data collection and interpretation. The sensor array should be planned to acquire large enough data set in order to conduct statistical analysis by varying distances and azimuths between sensor locations (Figure 11). Probe stands should not shadow or

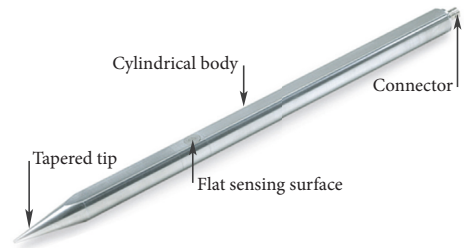

Figure 10: Pencil probe.

interfere with each other when placed in a row. Shadowing can be avoided by proper incrementing of sensor height and/or relative displacement between each. Fragmentation poles can be placed in front of a row of sensors along a radius to protect sensor from fragmentation impact and damage. After collecting, data (signal) needs to be transferred to the acquisition system that is usually situated several hundreds of meters from the blast site in some sort of protective structure (bunker). This is done usually by burying in the ground cables that could also be damaged or destroyed if not properly protected. During signal transmission distortions can occur which influence on data accuracy. In order to avoid signal distortions cables should be properly terminated preventing reflections at higher frequencies, i.e. proper attention should be directed to cable inductance and capacitance [93, 98].

2.7.2. Ground-Surface Transducer. Ground-surface transducers are probes used for measuring reflected blast pressures based on the principle of a pressure bar. Example of ground-surface transducer can be seen on Figure 12. The bar is acoustically impedance-matched to the tourmaline, resulting in a 1.5 MHz resonant frequency for the transducer [93]. The sensing face of the transducer must be levelled with the surface of the element in which they are mounted [94]. If the transducer should protrude from the surface, the protrusion will introduce errors by partially reflecting the blast wave. In some cases, deviations from flush mounting are required in order to isolate transducer from unwanted effects as high temperature interference. Alternately, if the transducer is recessed in the surface, the resultant acoustic cavity can act as a resonator [92, 95, 96]. These sensors are also susceptible to errors in measurements by environment influences, like high temperatures, intense light, element accelerations, etc. Mentioned influences are omitted by applying appropriate material as a

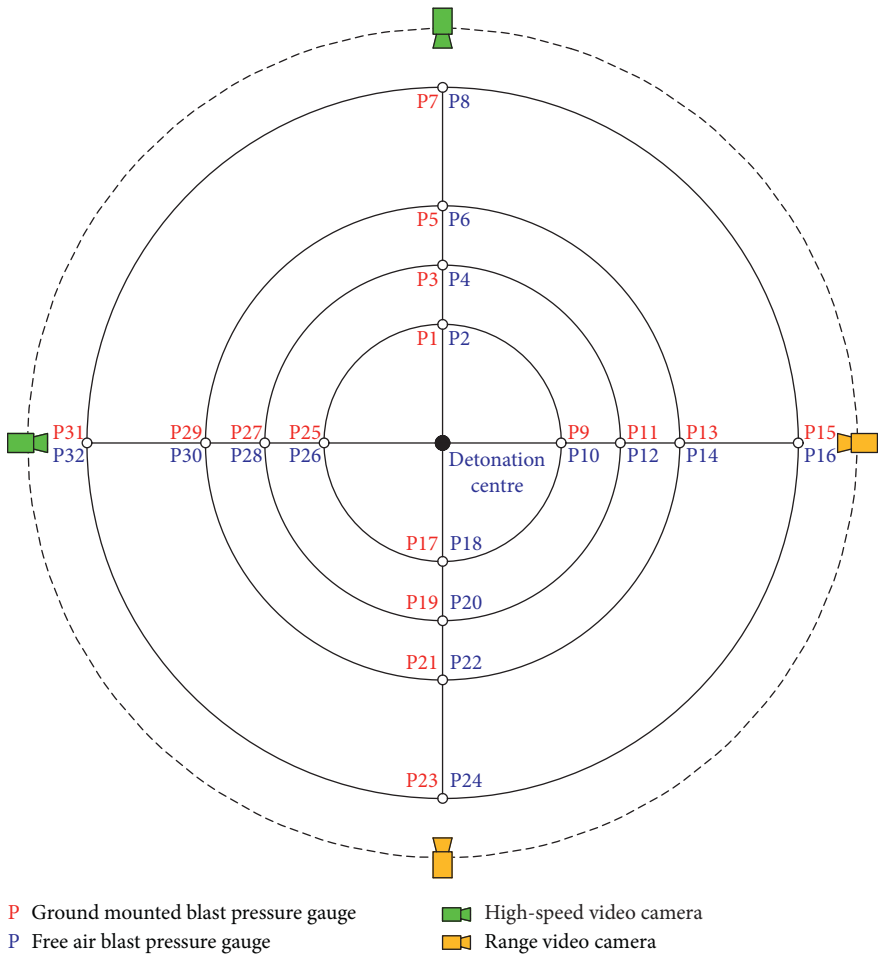

Figure 11: Scheme of the field blast sensors installation [91].

base, such as Teflon, Delrin or nylon in order to dampen unwanted accelerations, applying ceramic or rubber coating over the sensing face in order to prevent heat transfer, and applying opaque grease behind the screen on sensing face to block error signals due to intense light [91, 100]. Ground-surface transducers are not intended to record the entire pressure-time history but are limited to short record times. Longer record times require use of acceleration compensated pressure transducers but those are susceptible to thermal problems. The by-product of thermal induced housing expansion is negative signal residing after the blast event is clearly over. This is mitigated by use of ceramic or Room-Temperature-Vulcanizing silicone (RTV) coatings [100].

2.7.3. High-Speed Cameras. Useful instrument for monitoring specimen deformation in time is the high-speed camera. There are high-speed cameras with different capabilities in terms of sampling frequency, from 2000 Hz to 2000000 Hz (ultrahigh-speed camera) depending on the required usage [101]. Available recording time depends on sampling frequency, camera hard memory and photo resolution. Higher sampling frequency requires larger memory

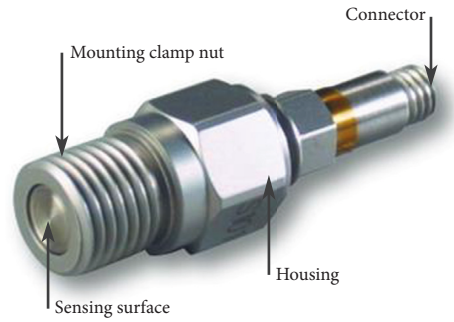

Figure 12: Ground-surface transducer.

for recording same event duration with same photo resolution than for lower sampling frequencies, respectively. Cameras used in blast measurements are typically positioned in safe distance in order to avoid damage by blast shock and/or fragment impact. They have limited capabilities if used for field blast tests in sense that the specimen is usually obscured by explosion fireball. Because of that camera usually is not capable of recording specimen behaviour, deformation and damage propagation. Nevertheless, with smart placement of the camera (for example behind the slab-like specimen opposite the explosion) it might be possible to record useful

data. Additionally, a special benefit of high-speed camera is possibility of calculating blast wave velocity from the recording that is then used to calibrate numerical simulations. In field tests, cameras can be used for recording blast fireball and wave expansion for further analysis. They are useful in other types of tests were camera has a clear view of the specimen, especially in shock tube tests where blast wave without any explosion by-products loads test specimen and blast simulator where specimen is loaded directly with hydraulic actuators.

3. Comparison to Numerical Simulations

To understand the behaviour of structures under blast loading, as stated before, full-scale blast tests would be the best course of action. However, these tests are limited due to security restrictions and a lack of the considerable resources required. Therefore, numerical modelling and simulation have recently been proven to be a valuable tool in simulating the behaviour of structures under blast loading [102–106]. Simulations are conducted using hydrocode software that is specialized numerical program for fluid dynamics. Table 6 gives a short list of conducted numerical simulations of blast effects on structural elements. Nonlinear dynamic blast analysis using hydrocodes [107–109] can be conducted using a 2D axis-symmetry simulation or a full 3D simulation. If 2D simulations are used, running times are reasonable and results are adequate but stiffer than the experimental results. In order to capture the true physics of the problem, 3D simulation can be applied because it resembles the actual situation. However, despite great advances in computation performance, there are still limitations when computing 3D simulations for blast analysis. Run times can be in order of days or weeks or even longer particularly when basic serial computing is used, but this can be somewhat reduced if parallel processing is applied. The numerical analysis of structures under irregular blast loading is also influenced by mesh geometries. This mesh size dependence is occurring due to gaps between the explosive energy and internal energy of structures and specific mechanical properties within the material model [3]. Numerical simulations can supply quantitative and accurate details of stress, strain, and deformation fields that are difficult to reproduce experimentally.

Hydrocode software can utilize several different numerical techniques: Eulerian, Lagrangian, arbitrary Lagrange Euler (ALE), and smoothed particle hydrodynamics (SPH) to optimise the analysis of nonlinear dynamic problems.

Dynamic response of a structure to an explosive detonation can be best described using the Eulerian approach for the explosive detonation while structural response is generally best modelled using a Lagrangian method. Solid continua and structures are usually modelled using a Lagrange processor which operates on a structured (I-J-K) numerical mesh consisting of either quadrilateral (2D) or solid (3D) elements depending on the type of analysis, planar or spatial, respectively. Main characteristic of the Lagrange processor is that the numerical mesh moves and distorts with the motion of material, and there is no transport of material from cell to cell. Such a shape has an advantage that the motion tracking of material is very accurate, and the material interface and free surfaces are clearly defined. Severe material deformations result in high numerical mesh distortions which can lead to loss of calculation accuracy and efficiency or even calculation failure. Fluid, gases, and large distortions are usually modelled using the Euler processor. It includes first-order and second-order accuracy schemes. Material flows through the fixed numerical mesh. The equations of mass, momentum, and energy conservation are solved through a control volume method. The advantage of such a scheme is that large material flows and distortions can be easily treated. Because material interfaces and free surfaces are not easily distinguished in this method, sophisticated techniques must be utilized in order to track material interfaces. This leads to a numerical solver that allows both solutions in a single simulation with coupling between these solvers in the temporal and spatial domains [3]. Most commonly used processor is the arbitrary Lagrange–Euler (ALE) processor that combines the best features of both methods. It is a hybrid processor that enables free numerical mesh movement and distortion in accordance with user conditions. The calculation procedure is supplemented with an additional computational step that moves the grid and remaps the solution onto a new grid. Smoothed particle hydrodynamics (SPH) is a numerical meshless method that does not need definition of nodes and elements, instead, only a collection of points (particles) is necessary to represent a given body (element). A prescribed set of continuum equations is discretized by interpolating the properties at a discrete set of points distributed over the solution domain using a fully Lagrangian modelling scheme. Its main advantage is the Lagrangian nature associated with the lack of a fixed mesh.

These employ partial differential equations that govern the basic physics principles of conservation of mass, momentum, and energy (Table 7). The equations to be solved are time-dependant and nonlinear. Constitutive models that describe material behaviour and a set of initial and boundary conditions together with differential equations define the complete system for blast analysis [3]. Numerical programs usually used in blast modelling, which are proved to provide most reliable results, are LS-DYNA [111], AUTODYN [112], and ABAQUS [113].

Due to material complex behaviour in blast analysis, a wide range of phenomena have to be modelled, for example, strain hardening, nonlinear pressure response, compaction, crushing, etc. Because of that, models are often broken into three components: equation of state, material strength model, and material failure model. An equation of state defines the hydrodynamic response of a material (important due to the air environment in which blast pressures are generated and through which are blast waves transferred to structures). Material strength models define nonlinear elastic-plastic response, and material failure models simulate the various ways in which materials fail. There is a wide range of predefined explicit material models available in each software material library.

Table 6: Numerical simulations used for calculating blast effects.

Test type	Author	Year	Element type	Software	Formulation	FE type	Symmetry	Mesh size (mm)
Field tests	Ohtsu et al. [23]	2007	Slab	BEM	N/A	N/A	N/A	N/A
	Wei et al. [12]	2007	Slab	ABAQUS	N/A	Solid, shell	Yes (1 : 4)	N/A
	Schenker et al. [9]	2008	Slab	LS-DYNA	N/A	Shell	N/A	N/A
	Wu et al. [86]	2011	Column	LS-DYNA	MM-ALE	Solid, beam	No	50
	Foglar and Kovar [17]	2013	Slab	LS-DYNA	N/A	Solid, beam	No	30 and 50
	Tabatabaei et al. [22]	2013	Slab	LS-DYNA	Lagrange	Solid, beam	No	N/A
	Zhao and Chen [14]	2013	Slab	LS-DYNA	N/A	Solid, beam	Yes (1 : 4)	N/A
	Castedo et al. [4]	2015	Slab	LS-DYNA	Lagrange	Solid, shell, beam	Yes (1 : 2)	15, 5 and 50
	Foglar et al. [18]	2015	Slab	LS-DYNA	N/A	Solid, beam	No	N/A
	Li et al. [24]	2015	Slab	LS-DYNA	SPH	Solid, beam	No	8 and 40
	Mao et al. [19]	2015	Slab	LS-DYNA	N/A	N/A	No	N/A
	Mazurkiewicz et al. [31]	2015	Column	LS-DYNA	Euler Lagrange MM-ALE	Shell	No	N/A
	Codina et al. [32]	2016	Column	AUTODYN	Euler Lagrange	Solid, beam	No	10
Shock tubes	Ellis et al. [10]	2014	Slab	ABAQUS	N/A	Solid	No	12.7 and 16
	Thiagarajan et al. [40]	2015	Slab	LS-DYNA	N/A	Solid, beam	No	25.4, 12.7 and 6.35
Blast pendulum systems	Heinchie et al. [63]	2014	Plate	ABAQUS	MM-ALE	Solid	No	N/A
	Fallah et al. [61]	2014	Plate	AUTODYN and ABAQUS	N/A	Solid	No	N/A
	Guan et al. [62]	2014	Plate	ABAQUS	N/A	Solid, shell	No	N/A
	Li et al. [65]	2014	Panel	AUTODYN	MM-ALE	Shell	Yes (1 : 4)	0.05
Blast simulator	Oesterle [75]	2009	Wall	LS-DYNA	Lagrange	Brick, beam, shell	No	N/A
	Stewart [77]	2010	Column	LS-DYNA	Lagrange	Shell	No	12.7
	Huson [72]	2012	Beam and plate	LS-DYNA	N/A	Continuum elements	No	N/A
	Li et al. [50]	2012	Column	LS-DYNA	N/A	N/A	No	N/A
	Stewart [78]	2012	Column	LS-DYNA	Lagrange	Shell	No	N/A
	Stewart [79]	2014	Column	LS-DYNA	Lagrange	Shell	No	12.7
	Stewart et al. [67]	2014	Column	LS-DYNA	Lagrange	Shell	No	N/A
Blast chambers	Wu et al. [70]	2013	Chamber	AUTODYN	Euler	N/A	No	10
	Snyman et al. [84]	2016	Chamber	AUTODYN	Euler Lagrange	N/A	axi	10 and 4

Table 7: Governing equations [104, 108, 110].

	Euler	Lagrange
Mass	$(d\rho/dt) + \rho(\partial u_i/\partial x_i) = 0$	$(\partial\rho/\partial t) + ((\partial/\partial x_i)(\rho u_i)) = 0$
Momentum	$du_i/dt = f_i + ((1/\rho)(\partial\sigma_{ij}/\partial x_j))$	$\partial u_i/\partial t = u_j(\partial u_i/\partial x_j) = f_i + ((1/\rho)(\partial\sigma_{ij}/\partial x_j))$
Energy	$di/dt = ((p/\rho^2)(d\rho/dt)) + (1/\rho)s_{ij}\dot{\varepsilon}_{ij}$	$(di/dt) + u_i(\partial i/\partial x_i) = ((p/\rho^2)((d\rho/dt) + u_i(\partial\rho/\partial x_j))) + ((1/\rho)s_{ij}\dot{\varepsilon}_{ij})$

where ρ represents the material density, u_i is the velocity, t time, x_i is the global Cartesian coordinate, σ_{ij} is the stress tensor, s_{ij} is the deviatoric part of stress tensor, p is the pressure (hydrostatic part of stress tensor), f_i is the external body force by unit mass, $\dot{\varepsilon}_{ij}$ is the deviatoric strain rate, and i is the specific internal energy.

Each model can be modified in order to better correspond to specific situation that is analysed. Blast load is modelled using detonation of high explosives that is initiated at specific point inside the defined explosive material. High explosives are modelled using Jones–Wilkins–Lee equation of state derived from cylinder test data [106]. One of the possible problems in numerical simulations of blast loading and interaction with structures is mesh size. Optimal mesh size is very difficult to obtain, and parametric study is often required in order to obtain balance

between result accuracy and calculation time [114]. Large mesh sizes can cause convergence issues and poor quality results, while small mesh size can cause prolonged calculation times, in scale of days or even weeks. This can be solved either by mesh size sensitivity analysis or by using parallel processing, or both.

Figure 9 in Wu et al. [86] represents comparison of experimentally tested and numerically simulated damage of RC column subjected to close-in detonation of charge equivalent to 25 kg of TNT. The computed crack profile of concrete as well as the large lateral deformations of longitudinal and transverse reinforcement is correctly reproduced if compared to the tested specimen.

Figure 9 in Castedo et al. [4] shows comparison of experimentally tested and numerically simulated damage of RC slab strengthened with steel plate on the upper side of the slab, directly under the explosive charge. A numerical model was developed in order to simulate the structural behaviour of full-scale RC slabs under blast loading. The numerical results were validated with experimental data in three field tests in which a standard RC slab was blasted under the same conditions. The extent of surface damage on each face was used to assess the performance of numerical modelling in comparison to tests. Conclusion was that the numerical models are able to predict the damage distributions successfully even when the test characteristics change. While these models are not perfect, they can be used to explore the feasibility of other slab reinforcement concepts prior to explosive testing and to model more complex structures affected by blast loads.

4. Conclusion

The most realistic representation of blast loading can be obtained only with full-scale field tests which best mimic real-life situations. Field tests are the most widespread method for blast experimentation but also the most dangerous; in addition, if full-scale field tests are conducted, then the costs of conducting this kind of tests are exponentially higher. Blast experimentation is usually conducted on scaled specimens what reduces the need for large explosive quantities and consequently lowers the overall danger of injury. Except field tests, researchers are trying to design tests that are able to produce blast-like action on experimental specimens with new procedures without using explosives. One of the examples is the BakerRisk blast simulator that uses dynamic actuators for inducing blast-like impulse loading. The simulator is capable of blast testing of all types of structural elements and large-scale complex specimens from which interaction of elements can be observed, which is important for force distribution and overall structure behaviour studies. Usually researchers are adopting the test method that is best suited for their resource capability.

Same instruments are used for blast measurements regardless of the experimental method used. In the course of years, instruments are developed and designed to be more robust, not only in their design in order to withstand high pressures and debris impact but also in their reliability to transmit recorded signals without any distortions.

Although blast phenomena can be difficult to model, because of the large number of variations in parameters which describe material models, finite element types and sizes, and boundary conditions and explosive loading, numerical models can be used to predict structural behaviour with fairly good accuracy in comparison to experimental tests. Use of advanced computer modelling (sophisticated material models, parallel processing, etc.) is essential to understand the behaviour of structures subjected to a blast load.

Further development of blast tests and measuring instruments can lead to better numerical representation of phenomena and consequently, maybe, to full substitution of field or any other kind of tests to numerical simulation. However, in order to achieve this, high reliability of accumulated test data and considerable speed-up of computer-processing capabilities have to be ensured.

Conflicts of Interest

The authors declare that there are no conflicts of interest regarding the publication of this paper.

Acknowledgments

This paper was supported in part by the Croatian Science Foundation (HRZZ) under the project (UIP-2017-05-7041) "Blast Load Capacity of Highway Bridge Columns," and support for this research is gratefully acknowledged.

References

[1] G. Morales-Alonso, D. A. Cendón, F. Gálvez, B. Erice, and V. Sánchez-Gálvez, "Blast response analysis of reinforced concrete slabs: experimental procedure and numerical simulation," *Journal of Applied Mechanics*, vol. 78, article 051010, 2011.

[2] M. Arlery, A. Rouquand, and S. Chhim, "Numerical dynamic simulations for the prediction of damage and loss of capacity of RC column subjected to contact detonations," in *Proceedings of 8th International Conference on Fracture Mechanics of Concrete Structures,* J. Van Mier, G. Ruiz, C. Andrade, and R. Yu, Eds., Toledo, Spain, March 2001.

[3] S.-H. Yun, H.-K. Jeon, and T. Park, "Parallel blast simulation of nonlinear dynamics for concrete retrofitted with steel plate using multi-solver coupling," *International Journal of Impact Engineering*, vol. 60, pp. 10–23, 2013.

[4] R. Castedo, P. Segarra, A. Alañon, L. M. Lopez, A. P. Santos, and J. A. Sanchidrian, "Air blast resistance of full-scale slabs with different compositions: numerical modeling and field validation," *International Journal of Impact Engineering*, vol. 86, pp. 145–156, 2015.

[5] S. Fujikura and M. Bruneau, "Experimental investigation of seismically resistant bridge piers under blast loading," *Journal of Bridge Engineering*, vol. 16, no. 1, pp. 63–71, 2010.

[6] P. F. Silva, B. Lu, and A. Nanni, "Prediction of blast loads based on the expected damage level by using displacement based method," in *Proceedings of First International Conference on Safety and Security Engineering (SAFE/05)*, Rome, Italy, June 2005.

[7] D. Yankelevsky, S. Schwarz, and B. Brosh, "Full scale field blast tests on reinforced concrete residential buildings-from

theory to practice," *International Journal of Protective Structures*, vol. 4, no. 4, pp. 565–590, 2013.

[8] M. A. Yusof, N. Norazman, A. Ariffin, F. Mohd Zain, R. Risby, and C. Ng, "Normal strength steel fiber reinforced concrete subjected to explosive loading," *International Journal of Sustainable Construction Engineering and Technology*, vol. 1, pp. 127–136, 2011.

[9] A. Schenker, I. Anteby, E. Gal et al., "Full-scale field tests of concrete slabs subjected to blast loads," *International Journal of Impact Engineering*, vol. 35, no. 3, pp. 184–198, 2008.

[10] B. D. Ellis, B. P. DiPaolo, D. L. McDowell, and M. Zhou, "Experimental investigation and multiscale modeling of ultra-high-performance concrete panels subject to blast loading," *International Journal of Impact Engineering*, vol. 69, pp. 95–103, 2014.

[11] N. Đuranović, "Eksperimentalno modeliranje impulsom opterećenih armiranobetonskih ploča," *Građevinar*, vol. 54, pp. 455–463, 2002.

[12] J. Wei, R. Quintero, N. Galati, and A. Nanni, "Failure modeling of bridge components subjected to blast loading part I: strain rate-dependent damage model for concrete," *International Journal of Concrete Structures and Materials*, vol. 1, no. 1, pp. 19–28, 2007.

[13] W. Wang, D. Zhang, F. Lu, S.-C. Wang, and F. Tang, "Experimental study on scaling the explosion resistance of a one-way square reinforced concrete slab under a close-in blast loading," *International Journal of Impact Engineering*, vol. 49, pp. 158–164, 2012.

[14] C. F. Zhao and J. Y. Chen, "Damage mechanism and mode of square reinforced concrete slab subjected to blast loading," *Theoretical and Applied Fracture Mechanics*, vol. 63–64, pp. 54–62, 2013.

[15] U. J. Alengaram, N. H. W. Mohottige, C. Wu, M. Z. Jumaat, Y. S. Poh, and Z. Wang, "Response of oil palm shell concrete slabs subjected to quasi-static and blast loads," *Construction and Building Materials*, vol. 116, pp. 391–402, 2016.

[16] C. Wu, D. Oehlers, M. Rebentrost, J. Leach, and A. Whittaker, "Blast testing of ultra-high performance fibre and FRP-retrofitted concrete slabs," *Engineering Structures*, vol. 31, no. 9, pp. 2060–2069, 2009.

[17] M. Foglar and M. Kovar, "Conclusions from experimental testing of blast resistance of FRC and RC bridge decks," *International Journal of Impact Engineering*, vol. 59, pp. 18–28, 2013.

[18] M. Foglar, R. Hajek, M. Kovar, and J. Štoller, "Blast performance of RC panels with waste steel fibers," *Construction and Building Materials*, vol. 94, pp. 536–546, 2015.

[19] L. Mao, S. J. Barnett, A. Tyas, J. Warren, G. Schleyer, and S. Zaini, "Response of small scale ultra high performance fibre reinforced concrete slabs to blast loading," *Construction and Building Materials*, vol. 93, pp. 822–830, 2015.

[20] C. Wu and J. Li, "Structural protective design with innovative concrete material and retrofitting technology," *Procedia Engineering*, vol. 173, pp. 49–56, 2017.

[21] D. Nicolaides, A. Kanellopoulos, P. Savva, and M. Petrou, "Experimental field investigation of impact and blast load resistance of ultra high performance fibre reinforced cementitious composites (UHPFRCCs)," *Construction and Building Materials*, vol. 95, pp. 566–574, 2015.

[22] Z. S. Tabatabaei, J. S. Volz, J. Baird, B. P. Gliha, and D. I. Keener, "Experimental and numerical analyses of long carbon fiber reinforced concrete panels exposed to blast loading," *International Journal of Impact Engineering*, vol. 57, pp. 70–80, 2013.

[23] M. Ohtsu, F. A. K. M. Uddin, W. Tong, and K. Murakami, "Dynamics of spall failure in fiber reinforced concrete due to blasting," *Construction and Building Materials*, vol. 21, no. 3, pp. 511–518, 2007.

[24] J. Li, C. Wu, and H. Hao, "Investigation of ultra-high performance concrete slab and normal strength concrete slab under contact explosion," *Engineering Structures*, vol. 102, pp. 395–408, 2015.

[25] T. Rodríguez-Nikl, *Experimental Simulations of Explosive Loading on Structural Components: Reinforced Concrete Columns with Advanced Composite Jackets*, University of California, San Diego, CA, USA, 2006.

[26] S. Fujikura, M. Bruneau, and D. Lopez-Garcia, "Experimental investigation of multihazard resistant bridge piers having concrete-filled steel tube under blast loading," *Journal of Bridge Engineering*, vol. 13, no. 6, pp. 586–594, 2008.

[27] S. Fujikura and M. Bruneau, "Blast resistance of seismically designed bridge piers," in *Proceedings of 4th World Conference on Earthquake Engineering*, p. 5, Beijing, China, October 2008.

[28] C. E. Davis, G. D. Williams, E. B. Williamson et al., "Design and detailing guidelines for bridge columns subjected to blast and other extreme loads," in *Proceedings of Structures 2009: Don't Mess with Structural Engineers © 2009 ASCE*, pp. 1–10, Austin, TX, USA, April 2009.

[29] E. B. Williamson, C. Holland, O. Bayrak, G. D. Williams, K. Marchand, and J. Ray, "Blast-resistant highway bridges: design and detailing guidlines," in *Proceedings of Structures Under Shock and Impact X*, p. 142, Washington, DC, USA, April 2008.

[30] S. Fujikura and M. Bruneau, "Dynamic analysis of multihazard-resistant bridge piers having concrete-filled steel tube under blast loading," *Journal of Bridge Engineering*, vol. 17, no. 2, pp. 249–258, 2011.

[31] L. Mazurkiewicz, J. Malachowski, and P. Baranowski, "Blast loading influence on load carrying capacity of I-column," *Engineering Structures*, vol. 104, pp. 107–115, 2015.

[32] R. Codina, D. Ambrosini, and F. de Borbón, "Experimental and numerical study of a RC member under a close-in blast loading," *Engineering Structures*, vol. 127, pp. 145–158, 2016.

[33] J. Xu, C. Wu, H. Xiang et al., "Behaviour of ultra high performance fibre reinforced concrete columns subjected to blast loading," *Engineering Structures*, vol. 118, pp. 97–107, 2016.

[34] R. Brun, *Shock Tubes and Shock Tunnels: Design and Experiments*, Shock Waves, Lyon, France, 2009.

[35] W. A. Martin, "A review of shock tubes and shock tunnels," Report No. ZR-658–050, General Dynamics, San Diego, CA, USA, 1958.

[36] A. Kiverin and I. Yakovenko, "On the mechanism of flow evolution in shock-tube experiments," *Physics Letters A*, vol. 382, pp. 309–314, 2018.

[37] Y.-L. Ning and Y.-G. Zhou, "Shock tubes and blast injury modeling," *Chinese Journal of Traumatology*, vol. 18, pp. 187–193, 2015.

[38] A. Stolz, K. Fischer, C. Roller, and S. Hauser, "Dynamic bearing capacity of ductile concrete plates under blast loading," *International Journal of Impact Engineering*, vol. 69, pp. 25–38, 2014.

[39] A. Klomfass, C. Mayrhofer, and C. Kranzer, "A new large shock tube with square test section for the simulation of blast events," in *Proceedings of 22nd Mabs Military Aspects of Blast and Shock*, Bourgese, France, November 2012.

[40] G. Thiagarajan, A. V. Kadambi, S. Robert, and C. F. Johnson, "Experimental and finite element analysis of doubly reinforced concrete slabs subjected to blast loads," *International Journal of Impact Engineering*, vol. 75, pp. 162–173, 2015.

[41] A. Haris, H. P. Lee, and V. B. C. Tan, "An experimental study on shock wave mitigation capability of polyurea and shear thickening fluid based suspension pads," *Defence Technology*, vol. 14, no. 1, pp. 12–18, 2018.

[42] G. Schleyer, M. Lowak, M. Polcyn, and G. Langdon, "Experimental investigation of blast wall panels under shock pressure loading," *International Journal of Impact Engineering*, vol. 34, no. 6, pp. 1095–1118, 2007.

[43] F. Toutlemonde, C. Boulay, and C. Gourraud, "Shock-tube tests of concrete slabs," *Materials and Structures*, vol. 26, no. 1, pp. 38–42, 1993.

[44] J. Magnusson, M. Hallgren, and A. Ansell, "Air-blast-loaded, high-strength concrete beams. Part I: experimental investigation," *Magazine of Concrete Research*, vol. 62, no. 2, pp. 127–136, 2010.

[45] L. Zhang, R. Hebert, J. T. Wright, A. Shukla, and J.-H. Kim, "Dynamic response of corrugated sandwich steel plates with graded cores," *International Journal of Impact Engineering*, vol. 65, pp. 185–194, 2014.

[46] H. Aoude, F. P. Dagenais, R. P. Burrell, and M. Saatcioglu, "Behavior of ultra-high performance fiber reinforced concrete columns under blast loading," *International Journal of Impact Engineering*, vol. 80, pp. 185–202, 2015.

[47] J.-Y. Lee, H.-O. Shin, D.-Y. Yoo, and Y.-S. Yoon, "Structural response of steel-fiber-reinforced concrete beams under various loading rates," *Engineering Structures*, vol. 156, pp. 271–283, 2018.

[48] D. N. Lacroix and G. Doudak, "Experimental and analytical investigation of FRP retrofitted glued-laminated beams subjected to simulated blast loading," *Journal of Structural Engineering*, vol. 144, no. 7, article 04018089, 2018.

[49] M. Poulin, C. Viau, D. N. Lacroix, and G. Doudak, "Experimental and analytical investigation of cross-laminated timber panels subjected to out-of-plane blast loads," *Journal of Structural Engineering*, vol. 144, no. 2, article 04017197, 2018.

[50] B. Li, A. Nair, and Q. Kai, "Residual axial capacity of reinforced concrete columns with simulated blast damage," *Journal of Performance of Constructed Facilities*, vol. 26, no. 3, pp. 287–299, 2012.

[51] X. Zhang, H. Hao, and Z. Wang, "Experimental study of laminated glass window responses under impulsive and blast loading," *International Journal of Impact Engineering*, vol. 78, pp. 1–19, 2015.

[52] J. S. Humphreys, "Plastic deformation of impulsively loaded straight clamped beams," *Journal of Applied Mechanics*, vol. 32, no. 1, pp. 7–10, 1965.

[53] N. Jones, T. O. Uran, and S. A. Tekin, "The dynamic plastic behavior of fully clamped rectangular plates," *International Journal of Solids and Structures*, vol. 6, no. 12, pp. 1499–1512, 1970.

[54] N. Jones, R. N. Griffin, and R. E. Van Duzer, "An experimental study into the dynamic plastic behaviour of wide beams and rectangular plates," *International Journal of Mechanical Sciences*, vol. 13, no. 8, pp. 721–735, 1971.

[55] G. N. Nurick and J. B. Martin, "Deformation of thin plates subjected to impulsive loading—a review part II: experimental studies," *International Journal of Impact Engineering*, vol. 8, no. 2, pp. 171–186, 1989.

[56] G. Langdon, W. Lee, and L. Louca, "The influence of material type on the response of plates to air-blast loading," *International Journal of Impact Engineering*, vol. 78, pp. 150–160, 2015.

[57] J. Shen, G. Lu, Z. Wang, and L. Zhao, "Experiments on curved sandwich panels under blast loading," *International Journal of Impact Engineering*, vol. 37, no. 9, pp. 960–970, 2010.

[58] B. McDonald, H. Bornstein, G. S. Langdon, R. Curry, A. Daliri, and A. C. Orifici, "Experimental response of high strength steels to localised blast loading," *International Journal of Impact Engineering*, vol. 115, pp. 106–119, 2018.

[59] A. G. Hanssen, L. Enstock, and M. Langseth, "Close-range blast loading of aluminium foam panels," *International Journal of Impact Engineering*, vol. 27, no. 6, pp. 593–618, 2002.

[60] G. Langdon, Y. Chi, G. Nurick, and P. Haupt, "Response of GLARE© panels to blast loading," *Engineering Structures*, vol. 31, no. 12, pp. 3116–3120, 2009.

[61] A. S. Fallah, K. Micallef, G. Langdon, W. Lee, P. Curtis, and L. Louca, "Dynamic response of Dyneema® HB26 plates to localised blast loading," *International Journal of Impact Engineering*, vol. 73, pp. 91–100, 2014.

[62] Z. Guan, A. Aktas, P. Potluri, W. Cantwell, G. Langdon, and G. Nurick, "The blast resistance of stitched sandwich panels," *International Journal of Impact Engineering*, vol. 65, pp. 137–145, 2014.

[63] T. F. Henchie, S. C. K. Yuen, G. Nurick, N. Ranwaha, and V. Balden, "The response of circular plates to repeated uniform blast loads: an experimental and numerical study," *International Journal of Impact Engineering*, vol. 74, pp. 36–45, 2014.

[64] L. Jing, Z. Wang, V. Shim, and L. Zhao, "An experimental study of the dynamic response of cylindrical sandwich shells with metallic foam cores subjected to blast loading," *International Journal of Impact Engineering*, vol. 71, pp. 60–72, 2014.

[65] X. Li, Z. Wang, F. Zhu, G. Wu, and L. Zhao, "Response of aluminium corrugated sandwich panels under air blast loadings: experiment and numerical simulation," *International Journal of Impact Engineering*, vol. 65, pp. 79–88, 2014.

[66] I. B. Ghoor, *The Response of Concave Singly Curved Fibre Reinforced Moulded Sandwich and Laminated Composite Panels to Blast Loading*, University of Cape Town, Cape Town, South Africa, 2018.

[67] L. K. Stewart, A. Freidenberg, T. Rodriguez-Nikl et al., "Methodology and validation for blast and shock testing of structures using high-speed hydraulic actuators," *Engineering Structures*, vol. 70, pp. 168–180, 2014.

[68] T. Rodriguez-Nikl, G. Hegemier, and F. Seible, "Blast simulator testing of structures: methodology and validation," *Shock and vibration*, vol. 18, no. 4, pp. 579–592, 2011.

[69] A. Freidenberg, A. Aviram, L. Stewart, D. Whisler, H. Kim, and G. Hegemier, "Demonstration of tailored impact to achieve blast-like loading," *International Journal of Impact Engineering*, vol. 71, pp. 97–105, 2014.

[70] C. Wu, M. Lukaszewicz, K. Schebella, and L. Antanovskii, "Experimental and numerical investigation of confined explosion in a blast chamber," *Journal of Loss Prevention in the Process Industries*, vol. 26, no. 4, pp. 737–750, 2013.

[71] J. C. Wolfson, *Blast Damage Mitigation of Steel Structures from Near-Contact Charges*, University of California, San Diego, CA, USA, 2008.

[72] P. Huson, *Experimental and Numerical Simulations of Explosive Loading on Structural Components: Composite Sandwich Connections*, University of California, San Diego, CA, USA, 2012.

[73] P. Huson, R. J. Asaro, L. Stewart, and G. A. Hegemier, "Non-explosive methods for simulating blast loading of structures with complex geometries," *International Journal of Impact Engineering*, vol. 38, no. 7, pp. 546–557, 2011.

[74] M. Gram, A. Clark, G. Hegemier, and F. Seible, "Laboratory simulation of blast loading on building and bridge structures," in *Proceedings of 9th International Conference on Structures Under Shock and Impact IX*, vol. 87, p. 12, Paris, France, June 2006.

[75] M. G. Oesterle, *Blast Simulator Wall Tests: Experimental Methods and Mitigation Strategies for Reinforced Concrete and Concrete Masonry*, 2009.

[76] M. G. Oesterle, G. A. Hegemier, and K. B. Morrill, "Response of concrete masonry walls to simulated blast loads," in *Proceedings of Structures Congress*, pp. 1277–1286, Austin, TX, USA, May 2009.

[77] L. K. Stewart, *Testing and Analysis of Structural Steel Columns Subjected to Blast Loads*, University of California, San Diego, CA, USA, 2010.

[78] L. K. Stewart, "Experimental and computational methods for steel columns subjected to blast loading," in *Proceedings of Structures Under Shock and Impact*, vol. 12, Kos, Greece, September 2012.

[79] L. K. Stewart, "Computational modeling of steel columns subjected to experimentally simulated blasts," *International Journal of Computational Methods and Experimental Measurements*, vol. 2, no. 3, pp. 225–242, 2014.

[80] K. W. King and J. H. Waclawczyk, "Blast containment chamber development and testing," in *Proceedings of ASME 2006 Pressure Vessels and Piping/ICPVT-11 Conference*, pp. 3–13, Vancouver, BC, Canada, July 2006.

[81] Z. Whenhui, X. Honglu, Z. Guangquan, and G. K. Schleyer, "Dynamic response of cylindrical explosive chambers to internal blast loading produced by a concentrated charge," *International Journal of Impact Engineering*, vol. 19, no. 9-10, pp. 831–845, 1997.

[82] C. Wu, D. J. Oehlers, J. Wachl et al., "Blast testing of RC slabs retrofitted with NSM CFRP plates," *Advances in Structural Engineering*, vol. 10, no. 4, pp. 397–414, 2007.

[83] C. Wu, R. Nurwidayati, and D. J. Oehlers, "Fragmentation from spallation of RC slabs due to airblast loads," *International Journal of Impact Engineering*, vol. 36, no. 12, pp. 1371–1376, 2009.

[84] I. M. Snyman, F. J. Mostert, and W. Grundling, "Design and commissioning of a semi-confined blast chamber," *Defense Technology*, vol. 12, no. 2, pp. 147–158, 2016.

[85] Z. Jiba, T. J. Sono, and F. J. Mostert, "Implications of fine water mist environment on the post-detonation processes of a PE4 explosive charge in a semi-confined blast chamber," *Defence Technology*, vol. 14, no. 5, pp. 366–372, 2018.

[86] K.-C. Wu, B. Li, and K.-C. Tsai, "Residual axial compression capacity of localized blast-damaged RC columns," *International Journal of Impact Engineering*, vol. 38, no. 1, pp. 29–40, 2011.

[87] K. S. Long, M. Kasmuri, A. S. Z. Hasan, and R. Hamid, "Dynamic increase factor of high strength concrete with silica fume at high strain rate loading," *Materials Science Forum*, vol. 857, pp. 299–304, 2016.

[88] W. J. Cantwell and J. Morton, "The impact resistance of composite materials—a review," *Composites*, vol. 22, no. 5, pp. 347–362, 1991.

[89] M. Zhang, H. J. Wu, Q. M. Li, and F. L. Huang, "Further investigation on the dynamic compressive strength enhancement of concrete-like materials based on split Hopkinson pressure bar tests. Part I: experiments," *International Journal of Impact Engineering*, vol. 36, no. 12, pp. 1327–1334, 2009.

[90] P. S. Bulson, *Explosive Loading of Engineering Structures*, CRC Press, Boca Raton, FL, USA, 2002.

[91] P. L. Walter, *Measuring Static Overpressures in Air Blast Environments*, PCB Piezotronics Inc., Depew, NY, USA, 2010.

[92] P. L. Walter, "Air-blast and the science of dynamic pressure measurements," *Sound and Vibration*, vol. 38, pp. 10–16, 2004.

[93] P. L. Walter, *Introduction to Air Blast Measurements-Part I*, PCB Piezotronics Inc., Depew, NY, USA, 2004.

[94] P. L. Walter, *Introduction to Air Blast Measurements-Part II: Interfacing the Transducer*, PCB Piezotronics Inc., Depew, NY, USA, 2004.

[95] P. L. Walter, *Shock and Blast Measurement-Rise Time Capability of Measurement System?*, PCB Piezotronics Inc., Depew, NY, USA, 2004.

[96] P. L. Silver, "Evaluation of air blast measurement technique," in *Proceedings of 75th Shock and Vibration Symposium*, Virginia Beach, VA, USA, October 2004.

[97] P. L. Walter, *Introduction to Air Blast Measurements-Part V: Alternate Technologies?*, PCB Piezotronics Inc., Depew, NY, USA, 2004.

[98] P. L. Walter, "Validating the data before the structural model," *Experimental Techniques*, vol. 34, no. 6, pp. 56–59, 2006.

[99] P. L. Walter, *Introduction to Air Blast Measurements-Part IV: Getting the Signal Down the Cable*, PCB Piezotronics Inc., Depew, NY, USA, 2004.

[100] P. L. Walter, *Introduction to Air Blast Measurements-Part III: Guaranteeing that Validated Pressure Measurements are Acquired*, PCB Piezotronics Inc., Depew, NY, USA, 2004.

[101] Photron USA, *Photron High Speed Cameras*, Photron USA Inc., San Diego, CA, USA, 2015.

[102] B. Luccioni, D. Ambrosini, and R. Danesi, "Blast load assessment using hydrocodes," *Engineering Structures*, vol. 28, no. 12, pp. 1736–1744, 2006.

[103] D. Miller, H. Pan, R. Nance, A. Shirley, and J. Cogar, "A coupled eulerian/Lagrangian simulation of blast dynamics," in *Proceedings of Implast Sem 2010 Fall Conference*, Providence, RI, USA, October 2010.

[104] S. Borve, A. Bjerke, M. Omang, and E. Svinsas, *A Comparison of AUTODYN and RSPH on Two-dimensional Shock Waves Problems*, Norweigian Defence Estates Agency, Oslo, Norway, 2009.

[105] T. C. Chapman, T. A. Rose, and P. D. Smith, "Blast wave simulation using AUTODYN2D: a parametric study," *International Journal of Impact Engineering*, vol. 16, no. 5-6, pp. 777–787, 1995.

[106] G. E. Fairlie, "The numerical simulation of high explosives using AUTODYN-2D and 3D," in *Proceedings of Institute of Explosive Engineers 4th Biannual Symposium*, Lisbon, Portugal, December 1998.

[107] C. E. Anderson Jr., "An overview of the theory of hydrocodes," *International Journal of Impact Engineering*, vol. 5, no. 1–4, pp. 33–59, 1987.

[108] G. S. Collins, *An Introduction to Hydrocode Modeling*, Applied Modelling and Computation Group, Imperial College London, UK, 2002.

[109] H. Draganić and D. Varevac, "Numerical simulation of effect of explosive action on overpasses," *Građevinar*, vol. 69, no. 6, pp. 437–451, 2017.

[110] P. Kohnke, *ANSYS Theory Manual, Release 12.0*, ANSYS Inc., Canonsburg, PA, USA, 2009.
[111] J. O. Hallquist, *LS-DYNA User's Manual*, Livermore software technology corporation, Troy, MI, USA, 2000.
[112] ANSYS, *ANSYS AUTODYN User's Manual*, ANSYS Inc., Canonsburg, PA, USA, 2010.
[113] H. D. Hibbitt, B. I. Karlsson, and E. P. Sorensen, *ABAQUS User's Manual Version 6.5*, ABAQUS Inc., Pawtucket, RI, USA, 2004.
[114] H. Draganić and D. Varevac, "Analysis of blast wave parameters depending on air mesh size," *Shock and Vibration*, vol. 2018, Article ID 3157457, 18 pages, 2018.